ELSEVIER

NeuroImage

www.elsevier.com/locate/ynimg
NeuroImage 41 (2008) 985–997

Enhanced frontal low and high frequency power and synchronization in the resting EEG of parkinsonian patients

Morteza Moazami-Goudarzi,[a,b,*] Johannes Sarnthein,[a,c] Lars Michels,[a] Renata Moukhtieva,[a] and Daniel Jeanmonod[a,c]

[a]*University Hospital Zurich, Laboratory for Functional Neurosurgery, CH-8091 Zurich, Switzerland*
[b]*Institute of Neuroinformatics, ETHZ/UNIZH, Winterthurerstrasse 190, 8057 Zurich, Switzerland*
[c]*Center for Integrative Human Physiology, University of Zurich, CH-0857 Zurich, Switzerland*

Received 27 December 2007; revised 28 February 2008; accepted 17 March 2008
Available online 1 April 2008

Oscillatory and coherent EEG activity is increasingly recognized as a fundamental hallmark of cortical integrative functions. We aimed to study deviations from the norm of different resting EEG parameters in Parkinson's disease (PD) patients.

We compared spectral parameters of the resting EEG of PD patients ($n = 24$, median age 67 years) to those of healthy controls ($n = 34$, median age 62 years).

On average, the patient group exhibited higher spectral power over the frequency range of 2–100 Hz, and the dominant peak was shifted towards lower frequencies. Maximal differences appeared in the 6–9 Hz theta band in all electrodes. Frontal electrodes contributed most to this difference in the 4–6 Hz theta, 12–18 Hz beta and 30–45 Hz gamma bands. On an individual basis, the combination of six spectral power band parameters discriminated between patient and control groups and 72% of all subjects were classified correctly. Using LORETA source analysis, the generators of this power difference were localized to fronto-insulo-temporal cortical areas in the theta and beta bands, and to interhemispheric frontal (supplementary motor area, SMA) and cingulate areas in the 30–45 Hz gamma band. We calculated spectral coherence between electrode pairs in a frontal, central and parietal region of interest (ROI). In the frontal ROI, coherence was enhanced significantly in the patient group in the theta, high beta and gamma bands. In the parietal ROI, patients showed lower coherence around 10 Hz.

We demonstrate a deviation from the norm of different resting EEG parameters in PD patients. This evidence can be integrated in the context of a pathophysiological chain reaction initiated in the substantia nigra and resulting in a cortical aberrant dynamics rooted in enhanced dysrhythmic thalamocortical interactions.

Keywords: Parkinson's disease; EEG oscillations; Synchronization; Localization; Thalamocortical system

Introduction

The pathophysiological mechanisms of Parkinson's disease (PD) can be traced back to a chain reaction starting in the substantia nigra, going through the basal ganglia, and finally affecting the frontal thalamocortical network. The main output of the basal ganglia is indeed via the pallidothalamic tract into the thalamus. Due to a reduction of dopamine in the striatum, increased neuronal activity of the internal part of the globus pallidus (GPi) (Albin et al., 1989; Beric et al., 1996; DeLong, 1990; Hutchison et al., 1994; Lozano et al., 1998; Magnin et al., 2000; Sterio et al., 1994), causes a tonic overinhibition of the pallidal-recipient thalamic relay cells leading to a thalamocortical dysrhythmic interplay, named thalamocortical dysrhythmia (TCD), characterized by an overproduction of thalamic low threshold calcium spike bursts and an increase in low and high frequency EEG power (Jeanmonod et al., 1996, 2001; Llinas, 1984; Llinas and Pare, 1994; Llinás et al., 2001; Llinás et al., 1999; Magnin et al., 2000; Volkmann et al., 1992, 1996).

In this context, studies of the EEG activity of parkinsonian patients can yield useful information collected from the last station before inadequate outputs are sent from the cortex to the motor periphery. A tight anatomical re-entrant and divergent thalamocortical organization (Jones, 2001; Llinás et al., 1999) as well as profuse cortico-cortical connections, both ubiquitous in the brain hemisphere, provide the basis for the oscillatory and coherent cortical EEG activity which is increasingly recognized as a fundamental

Abbreviations: BA, Brodmann area; EEG, electroencephalogram; FFT, fast Fourier transform; LORETA, low resolution electromagnetic tomography analysis; MEG, magnetoencephalogram; UPDRS, Unified Parkinson's Disease Rating Scale.

* Corresponding author. University Hospital Zurich, Laboratory for Functional Neurosurgery, CH-8091 Zurich, Switzerland. Fax: +41 44 255 8946.
E-mail address: mormo@ini.phys.ethz.ch (M. Moazami-Goudarzi).
Available online on ScienceDirect (www.sciencedirect.com).

1053-8119/$ - see front matter © 2008 Elsevier Inc. All rights reserved.
doi:10.1016/j.neuroimage.2008.03.032

hallmark of cortical integrative functions. In particular, a tight thalamocortical coupling has been shown in PD patients (Sarnthein and Jeanmonod, 2007). Increases in oscillatory function within local cortical regions appear as increase in scalp EEG spectral power, while enhanced synchronization between distributed cortical regions appear as enhanced coherence between EEG signals from distributed recording sites (Nunez et al., 1997).

It has been shown that EEG oscillations are abnormal in PD patients during performance of specific tasks. But interpretation of these studies is made difficult by the differences in task performance between studies, and mainly by the fact that we still lack sufficient knowledge of the anomalies of the resting EEG state in PD. Over the years, a few studies have looked at the EEG power spectra in PD patients, showing excess power in either all frequency bands (Tanaka et al., 2000), or only in specific frequency bands (Bosboom et al., 2006; Salenius et al., 2002; Stanzione et al., 1996; Stoffers et al., 2007), or a slowing of the occipital background rhythm (Soikkeli et al., 1991). The localization of the cortical generators at the source of this power excess has not yet been investigated in detail, except in one pioneering MEG work (Moran et al., 2004). While neural synchronization plays a fundamental role in many brain functions, in normal as well as pathological brain states (Schnitzler and Gross, 2005; Uhlhaas and Singer, 2006), only one study has investigated EEG coherence and its modulation by therapy in PD patients (Silberstein et al., 2005), but not as compared to controls.

The goal of the present work was thus the analysis in PD patients of several resting EEG parameters, namely power, source localization and inter-regional coherence, as compared to a healthy control group.

Methods

Patients

The patient group consisted of 24 patients (median age 67 years, range 56–85 years, 10 women, 14 men). Individual characteristics of patients are summarized in Table 1.

Twenty of the patients suffered from mixed forms of the disease, i.e. displayed different combinations of tremulent and akinetic manifestations. Our patient group is therefore a representative sample for the general distribution of symptoms described in PD, in which most patients display a combination of tremor and akinesia (Hughes et al., 1993). There was no clinical evidence of dementia in any of the patients.

Healthy controls

The healthy control group consisted of 34 subjects (median age 62, range 41–77 years, 10 women, 24 men). All control subjects were screened for health problems using a detailed health questionnaire. They had no current or previous history of relevant physical illness and no current regimen of any medication to affect their EEG.

EEG recording sessions

The study was approved by the Kanton Zurich ethics committee. All subjects, patients and controls were informed about the aim and the scope of the study and all gave written informed consent, according to the declaration of Helsinki. Subjects were seated in a dimly lit room shielded against sound and stray electric fields and were video-monitored. All EEGs were acquired in the morning between 9 and 12 in order to exclude an impact of circadian factors on the EEG. Recording sessions of patients and controls followed an interleaved schedule and the recording apparatus was continuously calibrated. Subjects refrained from caffeinated beverages on the day of recording to avoid a caffeine-induced theta decrease in EEG (Landolt et al., 2004). Since drowsiness may result in enhanced theta power, the vigilance of subjects was checked by monitoring EEG parameters, such as slowing of the alpha rhythm or appearance of spindles. In addition, at the end of the recording, subjects were asked if they were awake during the whole recording session.

Within each session, spontaneous EEG was recorded for 5 min while subjects rested with their eyes closed. Before each recording, subjects were instructed to assume a comfortable position in a chair. They were free to place their head on a chin-rest. Subjects were instructed to close their eyes, to place their fingers on their eyelids to reduce rolling eye movements and to relax but to stay awake. A modified Sternberg working memory task (Jensen et al., 2002) was given at the end of the recording session to all controls and to the patients ($N=10$) who were not impeded by motor limitations and/or tiredness.

EEG signals were measured using 60 Ag/AgCl surface electrodes, which were fixed in a cap at the standard positions according to the extended 10–20 system (Easycap, Herrsching, Germany). During recording, electrode CPz served as reference. Impedances were below 5 kΩ in all electrodes processed in the further analysis. We used two additional bipolar electrode channels as eye and EMG monitors. EEG signals were registered using the SynAmps EEG system (Neuroscan Compumedics, Houston, TX, 0.017 μV precision, sampling rate 250 Hz, 0.3–100 Hz analog band pass filter, −12 dB/octave) and continuously viewed on a PC monitor.

Data preprocessing and editing

Data were analysed offline using Matlab (The Matworks, Natick, MA) EEGLAB (http://sccn.ucsd.edu/eeglab; Delorme and Makeig, 2004) and custom scripts. The scalp EEG was re-referenced to the mean of the signals recorded at the ear lobes. We confirmed alertness of subjects during the recording session by checking for slowing of the alpha rhythm, slow rolling eye movements or increasing theta power (5–9 Hz). Data were inspected in 5 s epochs, and large muscle, eye movement or heart beat artifacts were removed. For editing purposes, muscle artifacts were considered significant if the underlying EEG rhythms were not clearly seen. The EEG was decomposed into independent components using blind separation (independent component analysis, ICA). After the removal of components containing eye movement, muscle artifacts or heart beats, the signal was reconstructed. This procedure resulted in more than 60 s of EEG (except for one patient with 40 s) for estimates of power spectral density and coherence (mean: 251 ± 80 s).

To investigate the effect of ICA component rejection, we compared PD and control power spectra in two approaches: 1) after visual artifact rejection only (before ICA) and 2) after additional ICA component rejection (after ICA). To test for significant differences between the two approaches we performed a repeated measure ANOVA, considering mean band powers as within-subject variables and groups as between-subject variables. None of the mean band powers delta ($F=2.39$, $p=0.128$), theta ($F=0.487$, $p=0.488$), alpha ($F=0.093$, $p=0.76$), low beta ($F=0.17$, $p=0.67$), high beta ($F=0.025$, $p=0.87$), and gamma ($F=0.05$, $p=0.81$) showed a statistically significant difference between the two approaches.

Table 1
Patient clinical details

Patient	Age (years)	Sex	Disease duration (years)	UPDRS II	UPDRS III	Symptom laterality L,R,RL,LR	Symptom type A,T,AT,TA	L-Dopa intake on the morning of EEG in mg	Daily dose intake in mg	Depression	Anxiety	Frustration	Suffering	Reduction of QL
1	78	Male	29	29	30	RL	AT	200	L-Dopa 600 mg, Ropinirol 1 mg	0	0	0	1	1
2	73	Male	13	17	19	LR	TA	200	L-Dopa 800 mg, Biperiden 4 mg	2	1	0	3	2
3	66	Female	10	14	16	L	TA	100	L-Dopa 100 mg	0	1	1	3	3
4	63	Female	1	11	10	R	TA	0	No medication	1	0	2	3	3
5	66	Male	11	5	10	LR	TA	200	L-Dopa 1000 mg, pramipexol 1.5 mg, Biperiden 2 mg, Amantadine 200 mg,	0	2	0	3	2
6	70	Male	6	35	25	LR	TA	200	L-Dopa 1000 mg, Clonazepam 0.25 mg	3	2	4	4	2
7	56	Female	12	24	12	RL	TA	100	L-Dopa 500 mg	0	0	0	2	2
8	77	Female	9	19	30	RL	TA	0	No medication	0	0	2	3	3
9	71	Male	3	10	15	L	TA	0	L-Dopa 600 mg, Primidone 250 mg	2	0	0	1	3
10	67	Female	15	21	40	LR	TA	250	L-Dopa 900 mg, Primidone 125 mg	2	2	0	3	4
11	70	Female	3	12	6	LR	A	150	L-Dopa 450 mg, Entacapone 200 mg	1	1	2	3	2
12	59	Male	12	9	7	RL	A	0	L-Dopa 600 mg	0	1	2	1	2
13	66	Male	5	17	22	L	TA	200	L-Dopa 600 mg, Ropinirol 2 mg	1	0	0	4	3
14	85	Female	4	16	19	RL	TA	0	No medication	2	0	1	3	3
15	63	Female	8	20	30	LR	TA	200	L-Dopa 800 mg, Ropinirol 1 mg, pramipexol 0.125 mg, Biperiden 1 mg	0	3	0	3	2
16	73	Female	12	5	12	RL	A	0	L-Dopa 800 mg	1	1	0	4	4
17	62	Male	6	9	11	R	TA	0	No medication	2	1	1	3	2
18	68	Male	8	12	13	LR	TA	300	L-Dopa 500 mg, Ropinirol 1 mg	2	1	0	2	3
19	64	Female	24	23	27	LR	TA	125	L-Dopa 900 mg	1	3	1	3	3
20	67	Male	7	15	19	RL	TA	150	L-Dopa 450 mg, Ropinirol 3 mg, Procyclidine 10 mg	0	1	1	3	4
21	58	Male	6	16	11	LR	AT	0	L-Dopa 600 mg	0	1	1	2	1
22	76	Male	1.5	10	20	R	TA	0	L-Dopa 400 mg	0	1	0	3	2
23	85	Male	11	5	12	RL	TA	200	L-Dopa 1000 mg	0	0	0	1	1
24	63	Male	13	32	17	RL	TA	300	L-Dopa 900 mg, Tolcapone 100 mg, Ropinirol 2 mg	0	0	1	2	2
Median	67.0		8.5	15.5	16.5			137.5		0.5	1.0	0.5	3.0	2.0
Mean	68.6		9.6	16.1	18.0			119.8		0.8	0.9	0.8	2.6	2.5

Symptom laterality: RL (bilateral, right dominant), LR (bilateral, left dominant), R (right), L (left), AT (akinetic and tremulent manifestations with akinetic dominancy), TA (tremulent and akinetic manifestations with tremulent dominancy), T (pure tremulent manifestation), and A (pure akinetic manifestation). Psychoemotional scales and Reduction of Quality of Life (QL): 0—no sign of problem, 1—light, 2—moderate, 3—marked, and 4—severe.

Power spectral analysis

The spectral analysis was performed with the multitaper method, which offers optimal spectral smoothing, i.e. it allows the trading of resolution in the frequency domain for reduced variance (http://www.chronux.org; Mitra and Pesaran, 1999). Power spectra were calculated with a window length of 5 s, fft length of 32 s, bandwidth parameter nw=2 and k=3 tapers.

Measures of synchronization

The magnitude squared coherence MSC_{xy} for two signals, x and y, is equal to the average cross-power spectrum P_{xy} normalized by the averaged power spectra of the signals $MSC_{xy}=|P_{xy}|^2/(P_{xx}P_{yy})$. Coherence spectra were calculated with a window length of 4 s, fft length of 16 s, bandwidth parameter nw=4 and k=3 tapers. Coherence assesses the strength of the linear relationship between two signals at every frequency f, and its value lies between 0 and 1. It estimates the degree to which phases and amplitudes are dispersed at the frequency of interest. $MSC_{xy}=0$ means phases and amplitudes are randomly dispersed among all epochs. Signals are perfectly coherent ($MSC_{xy}=1$) at a given frequency when they have both a constant phase difference φ and constant amplitude ratio over the time considered. In this case, phases of signals x and y are identical in all epochs, i.e. the two signals are completely phase-locked at this frequency. Following EEG convention, the term synchronization is used here for any phase-locked correlated signals, not only those with zero phase lag. In this sense, an enhancement of coherence signifies increased synchronization between two cortical sites.

As an alternative approach to measuring synchronization, the phase locking value (PLV) was proposed (Lachaux et al., 1999). In contrast to coherence, where the amplitudes of the signals play a role, in the calculation of the PLV only the angle of the phase of the cross-power spectrum enters the analysis. Since both PLV and coherence are common in the EEG literature, we calculated both for a comparison. Both measures gave equivalent results in the statistical analysis so that only coherence results are presented.

To avoid a loss of statistical power, neighbouring electrodes were combined into three topographical regions of interest (ROI). The frontal ROI comprises electrode sites AF3, AFz, AF4, F5, F3, F1, Fz, F2, F4, F6 (45 electrode pairs); the central ROI, FC5, FC3, FC1, FCz, FC2, FC4, FC6, C5, C3, C1, Cz, C2, C4, C6, CP5, CP3, CP1, CPz, CP2, CP4,CP6 (210 pairs) and the parietal ROI P5, P3, P1, Pz, P2, P4, P6, PO3, POz, PO4 (45 pairs). We excluded electrodes of the outer ring (FP1, FPz, FP2, AF8, F8, TP8, P8, PO8, O2, O1, PO7, P7, TP7, T7, FT7, F7, and AF7) to prevent artifacts induced by muscle activity and eye movements.

The coherence spectra between the signals from each pair of electrodes in a ROI were calculated. The spectra were transformed using log (1+x) to achieve normal distribution and then averaged.

Statistical analysis of spectra

For groupwise comparisons, the power and coherence spectra of the PD group and the healthy control group were compared with the non-parametric Wilcoxon test for each frequency point or for band-averaged values. Z-values are not corrected for multiple comparisons and are therefore to be considered as exploratory.

For classification of individual subjects into patient or control group, classical linear discriminant analysis (DA) was carried out on the basis of spectral band power as feature vector. In order to summarize the data and because spectra from all electrodes had similar shape and scale, we averaged the log-transformed spectra of all scalp electrodes for each subject. The DA determines the linear combination of parameters which best separate the two groups, in the sense that it maximizes the "between-to-within" variance ratio. Each subject was then assigned to the closest group based on this linear combination. For discrimination, cross-validation was used (SPSS version 11.5) such that the chance level of assigning a subject to the correct group was 50%. Exact 99% confidence intervals for the true proportions of correct classification using EEG parameters were calculated from tabulated values for the binomial distribution and we could check whether the chance level 50% was within or outside these confidence intervals.

LORETA imaging

To localize the cortical sources of scalp EEG activity we used low resolution electromagnetic tomography analysis (LORETA; http://www.unizh.ch/keyinst; Pascual-Marqui et al., 1994). We first calculated the cross-spectral density matrix using multitaper FFT. With a spatial over-smoothing of 10^{-4} the current source density was estimated for 2394 cortical voxels within the frequency bands given above (Frei et al., 2001). This procedure resulted in one 3D LORETA image for each subject for each frequency range.

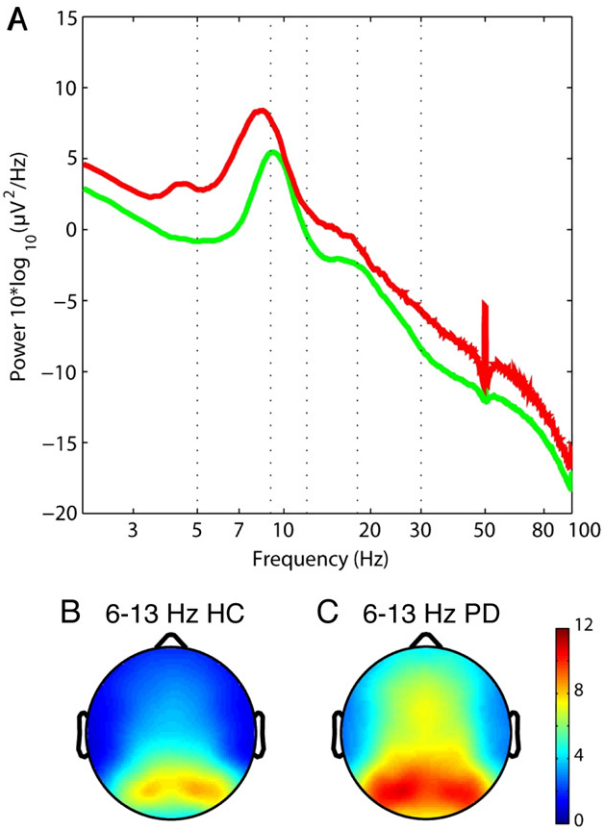

Fig. 1. Enhanced EEG power in PD patients. (A) In global EEG power the spectrum for the group of patients (red) was enhanced with respect to the group of healthy controls (green) and the dominant peak was shifted towards lower frequencies in the patient group. The topographical distribution of EEG power (6–13 Hz) on the scalp of control group (B) and patient group (C) had a maximum at parietal electrode sites, but extended to more frontal regions in the patient group.

LORETA images were statistically compared between groups through multiple voxel-by-voxel comparisons in a non-parametric test for functional brain imaging (Nichols and Holmes, 2002). The t values corresponding to $p<0.05$ or better were plotted onto a MRI template with a scale bar indicating statistical power and colour scale linearity equal to 75.

Results

Mean power spectra

In order to summarize the data and because spectra from all electrodes had similar shape and scale, we averaged the log-transformed spectra of all scalp electrodes for each subject. We then averaged these individual spectra to one spectrum for the patient group and one spectrum for the control group (Fig. 1). The patient group exhibited a higher dominant peak and more spectral power over the whole frequency range (2–100 Hz). The dominant peak was shifted towards lower frequencies ($p<0.001$). The distribution of band power across the patient and control group was significantly different ($p<0.01$) in the theta, low beta and gamma frequency bands.

In a comparison between medicated patients (who received L-Dopa in the 12 h before EEG recording session, $N=15$) and unmedicated patients (who received no L-Dopa during 12 h before EEG recording session, $N=9$, see Table 1), there were no significant differences in the spectral band power (delta, $p=0.07$, theta, $p=0.28$, alpha, $p=0.25$, low beta, $p=0.13$, high beta, $p=0.51$ and gamma, $p=0.55$).

We also investigated the effect of age or gender. There was neither significant interaction between age and group nor significant effect of age on different bands. Effect of age on different frequency bands was as follows: delta ($F=0.738$, $p=0.77$), theta ($F=0.746$, $p=0.76$), alpha ($F=0.639$, $p=0.86$), low beta ($F=0.63$, $p=0.86$), high beta ($F=0.732$, $p=0.77$) and gamma ($F=0.95$, $p=0.55$). For gender, there was neither significant interaction between gender and group nor significant effect of gender on different bands (delta: $F=7.57$, $p=0.34$; theta: $F=2.58$, $p=0.68$; alpha: $F=0.49$, $p=0.84$; low beta: $F=20.5$, $p=0.11$; high beta: $F=23.6$, $p=0.07$; gamma $F=4.4$, $p=0.55$).

Scalp power topography

After establishing a significant difference between patient and control group in spectra averaged over all electrodes, we were

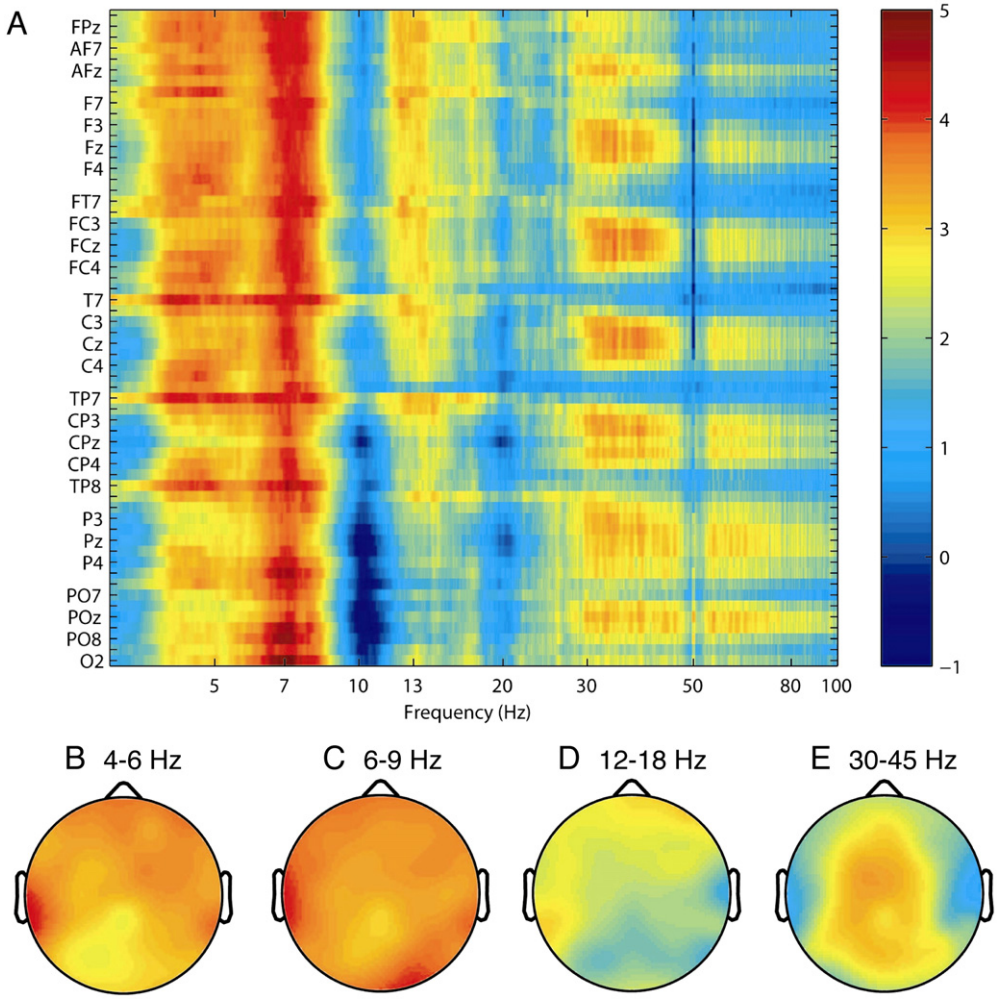

Fig. 2. Electrodewise comparison of power spectra. (A) Shown are Z-values for each electrode and frequency point (rank sum tests). (B) Between 4 Hz and 6 Hz, Z-values were maximal in centro-frontal sites with a tendency to frontal sites. (C) High Z-values occurred from 6 to 9 Hz in all electrodes. (D) Between 12 Hz and 18 Hz, Z-values were maximal in frontal electrodes. (E) Between 35 Hz and 45 Hz, Z-values were maximal in central electrodes.

interested to know which electrodes contributed most to this difference and at which frequency. We performed rank sum tests for each electrode at each frequency point and plotted the matrix of *Z*-values (Fig. 2A). In the 4–6 Hz band, high *Z*-values appeared in centro-frontal sites with predominance in frontal electrodes (Fig. 2B). Maximal *Z*-values appeared in the 6–9 Hz theta band

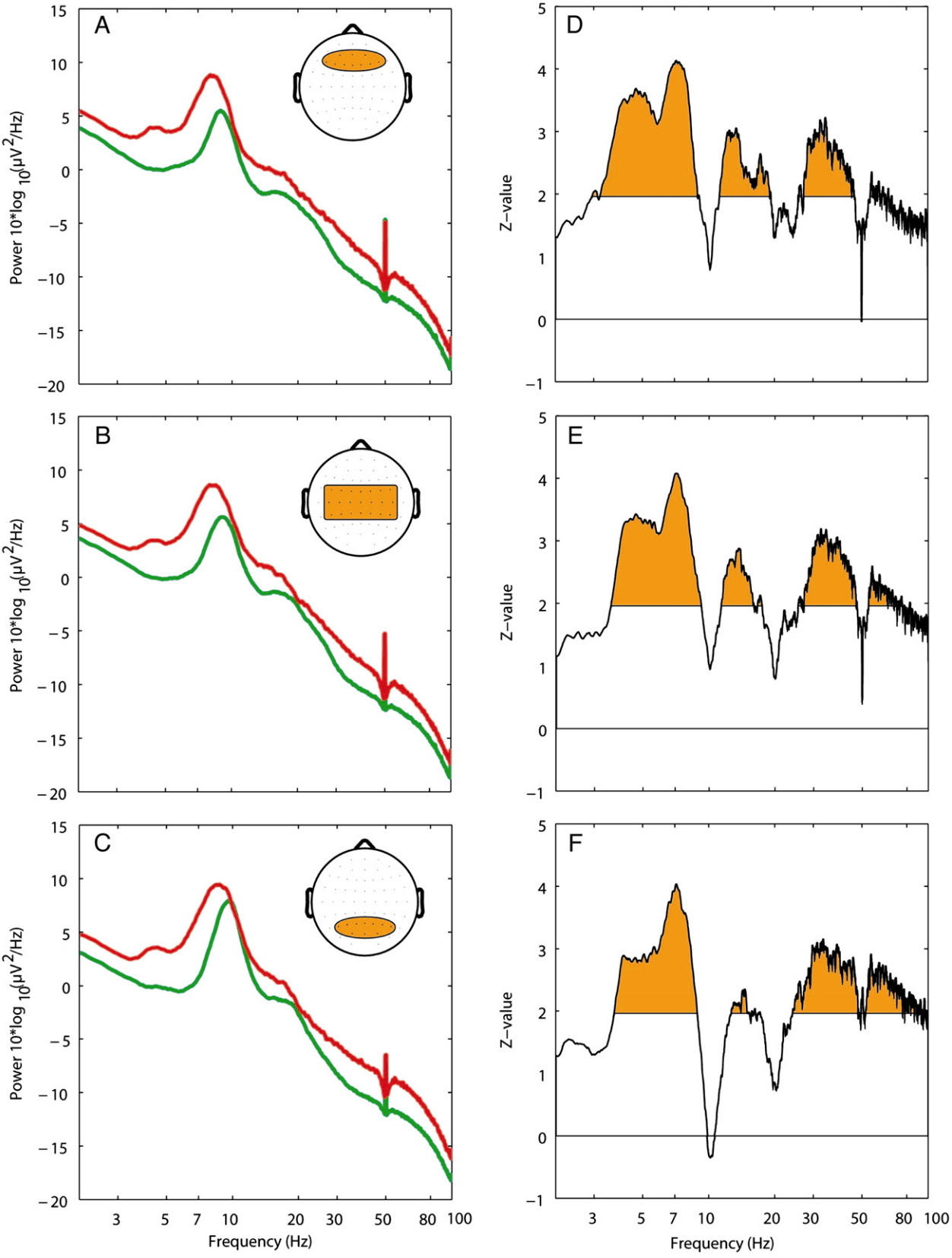

over the whole scalp (Fig. 2C). The frontal predominance was much more salient in the 12–18 Hz low beta band (Fig. 2D). In parietal electrodes, patients showed less power than controls around 10 Hz and around 20 Hz. In the gamma band around 40 Hz maximal power appeared in central electrodes (Fig. 2E).

For a complementary view, we averaged both power spectra and the spectra of *Z*-values in the frontal, central and parietal ROI (Fig. 3). In all ROIs, patients exhibited significantly enhanced power in several frequency ranges. Only in the parietal ROI did patients display reduced power in a narrow band around 10 Hz, which however, did not reach statistical significance (Fig. 3F). This reduction of power is related to the slowing in dominant frequency of PD patients (8.24 ± 1 Hz, mean ± standard deviation) with respect to healthy controls (9.24 ± 0.78 Hz). Due to the larger standard deviation of peak frequencies in patients, the group average spectrum exhibits a more rounded peak (Fig. 3C).

Coherence

The most striking result was the difference in coherence for different ROIs (Fig. 4). In the frontal ROI the patient group exhibited enhanced coherence in the theta, high beta and gamma frequency bands (Figs. 4A, D). In the central ROI no significant difference between patient group and control group was found (Figs. 4B, E). Finally, in the parietal ROI patients showed lower coherence around 10 Hz compared to healthy controls (Figs. 4C, F). Similar spectra and *Z*-values were obtained with the PLV as measure for synchronization (data not shown), indicating that the differences in synchronization are a robust phenomenon. Comparison of power and coherence spectra in Figs. 3 and 4 reveals that there are only few similarities between the two. This is the evidence that power and coherence parameters are at least partly independent from each other.

The amount of coherence due to volume conductance can be estimated as a function of electrode separation on an experimental and theoretical basis (Nunez and Srinivasan, 2006, pp. 381–396). If the distance between two electrodes falls between 5.5 and 17 cm, the coherence due to volume conductance is close to zero. We looked in the frontal ROI for the coherence between electrodes which belong to each hemisphere, ignoring the midline electrodes and thus defining two ROI subsets, one left and one right. Taking into account that the average head circumference for the control group is 57.3 and for the PD group 56.6, we estimated that the minimum and maximum interhemispheric distances between the electrodes of both ROIs are 6 and 16 cm, thus falling exactly into the interval of close-to-zero volume conductance. In Fig. 4D, the *Z*-values of the interhemispheric coherences is shown in blue and reveals an unchanged coherence in theta, and only a reduction of the significant coherence increase in the gamma domain. We may therefore propose that the amount of observed interhemispheric increased coherence in the frontal ROI in the theta and beta domains is not significantly due to volume conductance. Additionally, we analysed the coherence values inside the two frontal ROI subsets, and found in the theta domain on the right side only a significant coherence increase, to be taken as an indication for a coherence asymmetry between the two frontal areas.

LORETA source localization

Generators of differential power are shown as activation in statistical maps for specified frequency ranges (Fig. 5). The enhanced spectral EEG power of the patient group is reflected in cortical overactivation in different frequency ranges spread over premotor, supplementary motor (SMA), cingulate motor, prefrontal dorsolateral and medial, orbitofrontal, frontopolar, insular and temporopolar cortices.

Discriminant analysis (DA)

To distinguish between the 24 patients and 34 controls on an individual basis, we performed a DA with the mean band power in six frequency bands as feature vector. The set of bands was optimized with respect to discriminative power starting from a set of arbitrary band edges, for which DA was calculated. Single band edges were shifted iteratively and the classification rate was determined for each iteration. This optimization procedure resulted in the optimal set of frequency bands delta (2–5 Hz), theta (5–9 Hz), alpha (9–12 Hz), low beta (12–18 Hz), high beta (18–30 Hz) and gamma (30–100 Hz). Interestingly, this set of frequency bands is close to the conventional sets of bands used in the EEG literature.

The different frequency bands contribute to the classification of the DA to different extent as described by the structural matrix. The contributions of the different bands decreased in the order theta, delta, low beta, gamma, high beta, and alpha. As a 2-dimensional illustration, Fig. 6 shows band power in theta and low beta for each subject. There is a tendency for patients (red crosses) and healthy controls (green circles) to appear as two clusters separated by the black discriminant line. If the whole feature vector of band power was used, 44 of all 58 subjects were classified correctly to either patient or control group. This corresponds to a classification rate of 72% with 99% confidence interval 55–86%. Since cross-validation was used to estimate the classification rate and the confidence interval excludes the 50% level (chance level), our result is significant with error probability $p < 0.01$.

Since we use DA for binary classification of subjects based on EEG parameters, we can statistically evaluate the usefulness of the method. The proportion of correctly classified subjects in the healthy control group gives a specificity of 82%. The proportion of correctly classified subjects in the patient group amounts to a sensitivity of 67%. Both parameters delineate the diagnostic power of EEG spectral analysis in PD. While of course PD is diagnosed clinically, the diagnostic power underlines the strength of the effects of PD on the scalp EEG.

Discussion

The most striking finding of this study in the EEG spectra of the patient group is the enhanced delta, theta, beta and gamma power (Fig. 1), with a slowing of the dominant peak. The analysis of individual spectra by DA substantiated the difference in EEG between PD patients and healthy controls on a statistical basis. While an altered state of cortico-cortical synchronization has been reported for a large variety of pathological brain states (Benedetti

Fig. 3. Comparison of power spectra for three ROIs. Power spectra for the group of patients (red) and the group of healthy controls (green) in the frontal ROI (A), central ROI (B) and parietal ROI (C). Insets: Shaded area includes electrodes of ROI. The power spectra of patients and controls were compared by a ranksum test for each frequency point for the frontal ROI (D), central ROI (E), and parietal ROI (F). Areas are shaded with $|Z| > 1.96$ corresponding to $p < 0.05$. Significant differences appear in delta, theta, low beta and gamma bands in the frontal ROI and the central ROI. For the parietal ROI significant differences appear in delta, theta and gamma bands. There is a trend towards reduced alpha power around 10 Hz in patients.

et al., 2006; Uhlhaas and Singer, 2006), we now report enhanced resting frontal EEG coherence in a group of PD patients with respect to a group of healthy controls (Figs. 4A, D). Our results are valid for PD in general, since the majority of our patients suffer from a combination of tremor and akinesia (Table 1) which is typical for PD (Hughes et al., 1993).

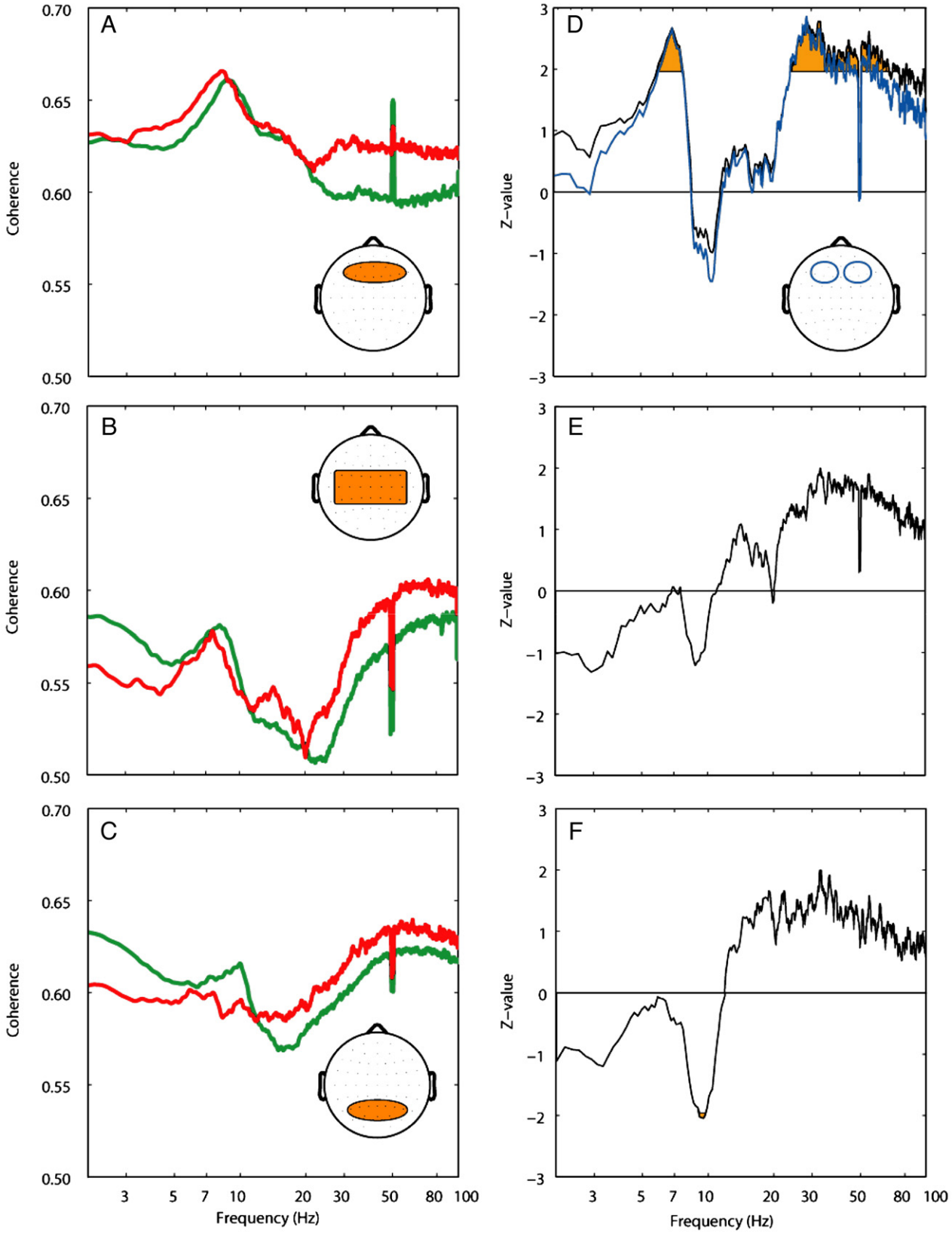

From a physiological point of view, spectral power in the EEG describes the activity of the dipole-like dendrites of cortical pyramidal cells arranged in parallel and space-averaged over an area of several cm^2 of cortex (Nunez et al., 2001), approximately underlying the electrode site (Pascual-Marqui et al., 2002). Coherence, however, estimates the degree of synchronization between the neuronal activities in two areas of cortex underlying two different electrodes (Nunez et al., 2001). Therefore power and coherence are thought to describe largely independent aspects of brain function.

Power

The general increase of power in patients (Fig. 1) is in line with a previous report of excess power in all frequency bands (Tanaka et al., 2000) and at variance with other reports of excess power only in specific frequency bands (Bosboom et al., 2006; Neufeld et al., 1994; Salenius et al., 2002; Stanzione et al., 1996; Stoffers et al., 2007). The general increase in power is confirmed if individual electrodes are analysed (Fig. 2A). Only for parietal electrodes a trend appeared for reduced power in the patients (Fig. 3F). This relative reduction is probably related to the shift of the dominant peak towards lower frequencies in the patient group (Fig. 3C) (Soikkeli et al., 1991).

The variance with some of the earlier reports may possibly be due to 1) our use of absolute power, while other authors use relative power with some special normalization, 2) the size of the patient group or the selection of patients in the different studies, and 3) the specific choice of frequency bands entering the statistical analysis, our analysis being less likely to be biased in this respect, since *Z*-values are calculated for each frequency point.

Although stronger increases of low frequency production were noted in demented as compared to non-demented PD patients (Caviness et al., 2007; Neufeld et al., 1994; Soikkeli et al., 1991), the latter were shown to have EEG power increases in the low frequency domain (Neufeld et al., 1994; Soikkeli et al., 1991; Stoffers et al., 2007) or in all frequency bands (Tanaka et al., 2000) in comparison with controls. In this study, there were no obvious clinical signs of dementia, and we did not perform detailed cognitive tests in all patients. The performance in a working memory task of ten patients was not significantly ($p=0.13$) different from controls. We may thus assume that the majority of the observed EEG changes are related to the motor PD state, without excluding the possibility of a partial effect due to mild to moderate cognitive deficits.

In addition we found an increase of beta (Tanaka et al., 2000) and gamma activities in our patients group, which we hypothesize to be due to the chronicity and severity of the disease. This hypothesis is in line with the concept of TCD (Jeanmonod et al., 2001; Llinás et al., 2001, 1999; Llinas et al., 2005), which entails an overproduction of low and high frequencies, the first being the cause of the second through the mechanism called edge effect (Llinas et al., 2005). The increased high frequency production in the SMA, at the end of the TCD process, may be seen as most directly related to the appearance of the motor manifestations of the disease.

The question may arise as to why the observed power increase extends over the whole frequency range. Two steps are to be considered in this context. The first one is the assumption of a correlation between the increased production of thalamic low threshold calcium spike bursts at ~4 Hz (Jeanmonod et al., 1996; Magnin et al., 2000) and the theta power increase. The second is the causal relationship between low and high frequency over-activities by means of the edge effect. The complex integration inside cortical columns in dialog with thalamus and with other cortical areas may explain a spreading of frequency overproductions around 4 Hz in the low frequency domain (thalamocortical integration) and into high frequencies through the edge effect (cortico-cortical integration).

Cortical generators of excess EEG power

In the theta band, the cortical generators of excess EEG power were located in widespread fronto-insulo-temporal areas, similar to what others have found with MEG (Llinas, personal communication). Such a localization speaks for a dysrhythmic co-involvement of associative and paralimbic areas in the pathogenesis of PD, which makes sense in view of the topographic and functional vicinity of prefrontal areas with premotor and motor domains. The pallidal-recipient thalamic nucleus ventral anterior, for example, is anatomically connected to premotor but also prefrontal associative areas. In addition, the importance of reactive emotional factors in PD (Aufenberg et al., 2007) is supported by the anxiodepressive ratings or our patient population (Table 1). Whether the cause of excess frontal theta power is lesional (related to dopamine loss) or functional (reactive to the fact of being affected by PD), the primary relevance of the whole cognitive-emotional network is anyway impressively pointed to by a recent report demonstrating massive reductions of motor PD manifestations during REM sleep (De Cock et al., 2007).

In the gamma band, the peak over activation was located in BA 6 in the medial frontal gyrus, corresponding to the supplementary motor area (SMA), well known as a relevant area for PD (Carbon et al., 2007; Huang et al., 2007; Turner et al., 2003).The importance of beta/gamma activity for motor action in the EEG is well documented for healthy subjects (Neuper and Pfurtscheller, 2001; Svoboda et al., 2004) and also in PD patients (Brown and Marsden, 1999; Llinás et al., 1999; Pfurtscheller et al., 1998; Schnitzler and Gross, 2005; Timmermann et al., 2003).

Coherence

We found enhanced coherence for theta and high beta/gamma band in the frontal ROI of the PD group (Figs. 4A, D). The low frequency maximum in the frontal spectrum of *Z*-values appears around ~7 Hz (Fig. 4D). This coincides with the finding of a maximal thalamocortical coherence to frontal electrodes (Sarnthein and Jeanmonod, 2007). The cortico-cortical and thalamocortical coupling is in agreement with the larger network of coherently active brain areas proposed for PD patients (Schnitzler and Gross, 2005). As for the high frequency maximum in the frontal spectrum of *Z*-values (Fig. 4D), coherence in a similar frequency range was found to be reduced when motor symptoms were reduced by therapeutic measures

Fig. 4. Comparison of coherence spectra for ROIs. Coherence spectra for the group of patients (red) and the group of healthy controls (green) in the frontal ROI (A), central ROI (B) and parietal ROI (C). Insets: Shaded area includes electrodes of ROI. In the frontal ROI, the blue circles display a right and a left electrode subset. The coherence spectra of patients and controls were compared by a ranksum test for each frequency point and areas with $|Z|>1.96$ corresponding to $p<0.05$ were shaded. Significant differences appear in theta and gamma in the frontal ROI. The blue curve shows the *Z*-values for the interhemispheric comparison of coherence in the frontal ROI (D). In the central ROI there is no significant difference between two groups (E). In the parietal ROI patients show reduced coherence which is significant around 10 Hz (F).

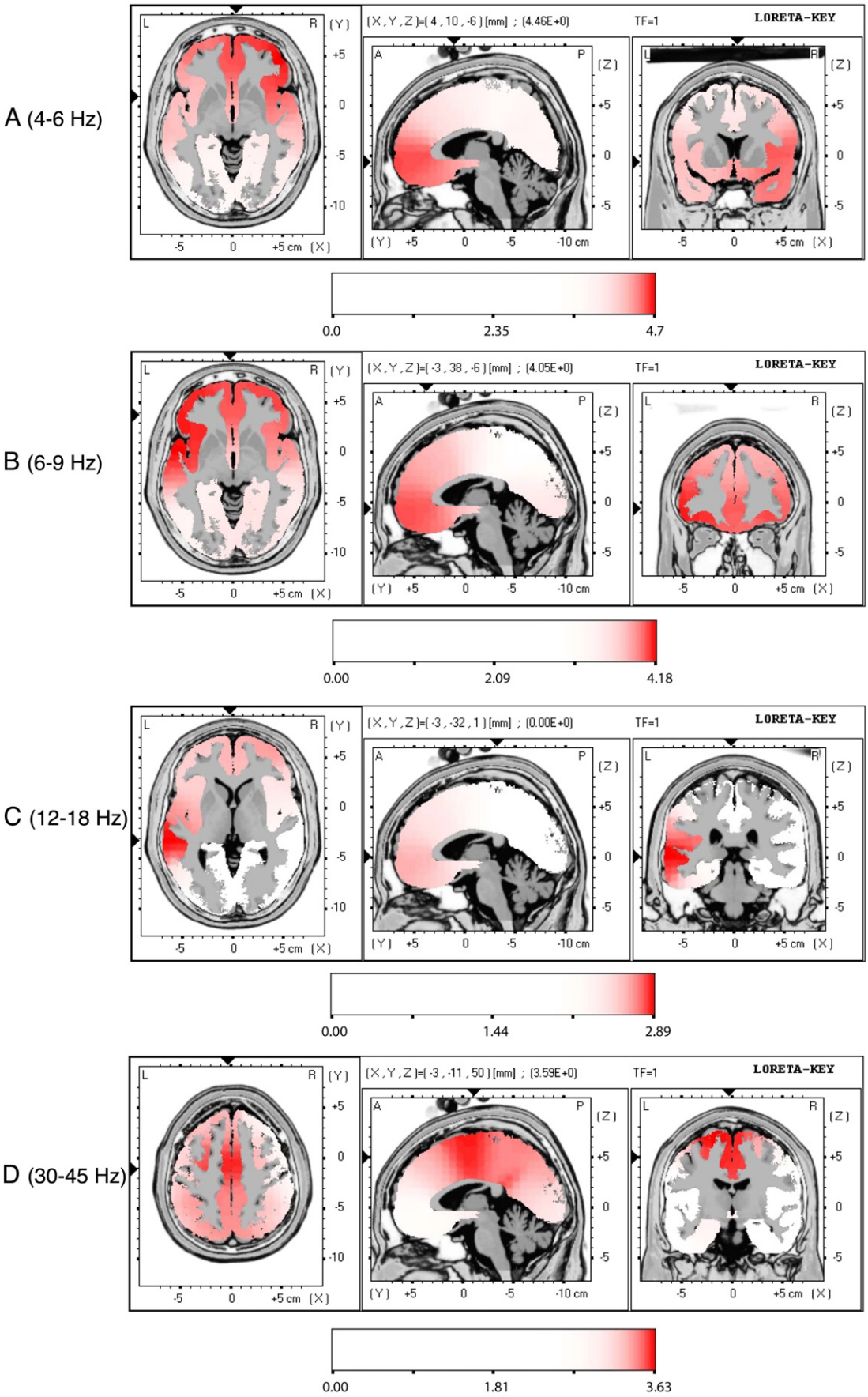
A (4-6 Hz)
(X,Y,Z)=(4 , 10 , -6) [mm] ; (4.46E+0)
TF=1
LORETA-KEY
0.0
2.35
4.7
B (6-9 Hz)
(X,Y,Z)=(-3 , 38 , -6) [mm] ; (4.05E+0)
TF=1
LORETA-KEY
0.00
2.09
4.18
C (12-18 Hz)
(X,Y,Z)=(-3 , -32 , 1) [mm] ; (0.00E+0)
TF=1
LORETA-KEY
0.00
1.44
2.89
D (30-45 Hz)
(X,Y,Z)=(-3 , -11 , 50) [mm] ; (3.59E+0)
TF=1
LORETA-KEY
0.00
1.81
3.63

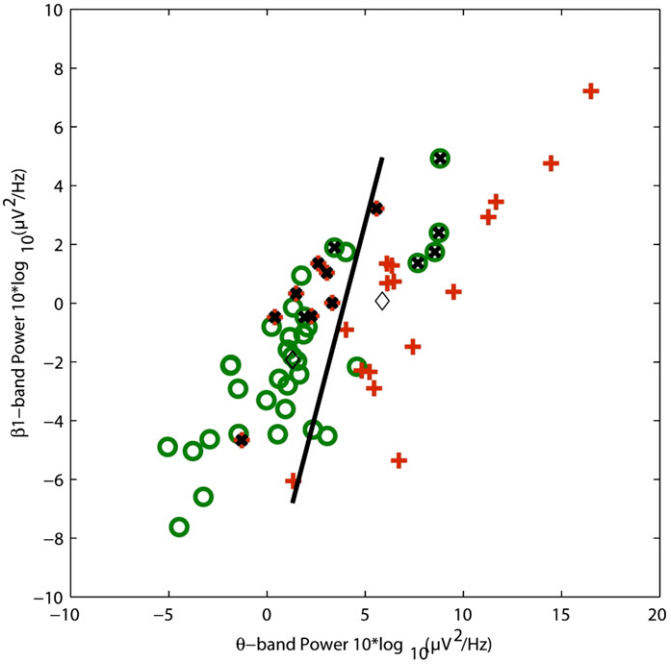

Fig. 6. Individual subject EEG spectral parameters. For each subject of the patient group (red crosses +) and the control group (green circles ○) theta band power is plotted against low beta (beta 1) band power. The group centers (diamonds) and black discriminant line result from a bivariate discriminant analysis (DA) using only low beta and theta band power. We also used the power in six frequency bands as feature vector for DA (misclassified subjects: "x"). Discriminative power was enhanced and 72% of all subjects were classified correctly.

(Silberstein et al., 2005). This indicates that high coherence in this frequency range is directly involved in the production of PD symptoms.

In the parietal ROI we found a reduction of coherence in patients around ~10 Hz (Figs. 4C, F). Together with the reduced parietal alpha power (Figs. 3C, F), this may be evidence that the normal process generating alpha activity is altered in patients.

Conclusion

We have demonstrated a low and high frequency EEG power and coherence increase in PD patients. The low frequency excess power could be localized in broad and bilateral fronto-insulo-temporal areas, speaking for an involvement of paralimbic and associative domains in the pathogenesis of PD. Gamma overactivation was found centered on the SMA, in good accordance with accepted cortical localizations in PD. An excess frontal inter-regional synchronization was also found, well compatible with a state of low frequency overactivity. We may thus postulate a persistent and deleterious state of EEG overactivity in the resting EEG of PD patients. These results can all be integrated into the TCD framework, which may be profiled as a pathophysiological chain reaction initiated in the substantia nigra and comprising an overinhibition of the premotor thalamus by the pallidum, the resulting increased production of thalamic low threshold calcium spike bursts, the increased generation of low frequency EEG activities, and finally, through the edge effect, a resulting high frequency overproduction. The low frequency activation may be proposed to relate to the appearance of motor negative symptoms (like akinesia), whereas the high frequency activation with the positive motor manifestations (like tremor).

Acknowledgments

We thank Jim Dodd for his help with the EEG recordings, Anne Morel for encouraging support and critical readings of the manuscript and Vera Bügler for secretarial work. We gratefully acknowledge financial support by Neuroscience Center Zurich and by Swiss National Foundation (3200B0-110028).

References

Albin, R.L., Young, A.B., Penney, J.B., 1989. The functional anatomy of basal ganglia disorders. Trends Neurosci. 12, 366–375.

Aufenberg, C., Sarnthein, J., Morel, A., Rousson, V., Gallay, M., Jeanmonod, D., 2007. A revival of Spiegel's campotomy: long term results of the stereotactic pallidothalamic tractotomy against parkinsonian thalamocortical dysrhythmia. Thalamus Related Syst. 1, 1–12.

Benedetti, F., Arduino, C., Costa, S., Vighetti, S., Tarenzi, L., Rainero, I., Asteggiano, G., 2006. Loss of expectation-related mechanisms in Alzheimer's disease makes analgesic therapies less effective. Pain 121, 133–144.

Fig. 5. Comparison of functional tomographic maps. LORETA functional images show differences in regional brain activity between patient group and healthy control group for three frequency ranges. For each frequency range, three orthogonal slices through the location of maximal increase are displayed. Images are colour coded ($p<0.01$, corrected for multiple comparison; linearity=75) registered to the stereotaxic Talairach space, and overlaid on a structural MRI scan. The MNI (Montreal Neurological Institute) coordinates are given on the slice maps. At cortical voxels, t values are colour coded according to the scale bar. Red areas correspond to overactivation in the patient group. Peak overactivations are localized to fronto-insulo-temporal cortex in the 4–6 Hz theta band (A) and the 6–9 Hz alpha band (B) and the 12–18 Hz beta band (C) and to medial central cortex in the 35–45 Hz gamma band (D).

Beric, A., Sterio, D., Dogali, M., Fazzini, E., Eidelberg, D., Kolodny, E., 1996. Characteristics of pallidal neuronal discharges in Parkinson's disease patients. Adv. Neurol. 69, 123–128.

Bosboom, J.L., Stoffers, D., Stam, C.J., van Dijk, B.W., Verbunt, J., Berendse, H.W., Wolters, E.C., 2006. Resting state oscillatory brain dynamics in Parkinson's disease: an MEG study. Clin. Neurophysiol. 117, 2521–2531.

Brown, P., Marsden, C.D., 1999. Bradykinesia and impairment of EEG desynchronization in Parkinson's disease. Mov. Disord. 14, 423–429.

Carbon, M., Felice Ghilardi, M., Dhawan, V., Eidelberg, D., 2007. Correlates of movement initiation and velocity in Parkinson's disease: a longitudinal PET study. Neuroimage 34, 361–370.

Caviness, J.N., Hentz, J.G., Evidente, V.G., Driver-Dunckley, E., Samanta, J., Mahant, P., Connor, D.J., Sabbagh, M.N., Shill, H.A., Adler, C.H., 2007. Both early and late cognitive dysfunction affects the electroencephalogram in Parkinson's disease. Parkinsonism Relat. Disord. 13, 348–354.

De Cock, V.C., Vidailhet, M., Leu, S., Texeira, A., Apartis, E., Elbaz, A., Roze, E., Willer, J.C., Derenne, J.P., Agid, Y., Arnulf, I., 2007. Restoration of normal motor control in Parkinson's disease during REM sleep. Brain 130, 450–456.

DeLong, M.R., 1990. Primate models of movement disorders of basal ganglia origin. Trends Neurosci. 13, 281–285.

Delorme, A., Makeig, S., 2004. EEGLAB: an open source toolbox for analysis of single-trial EEG dynamics including independent component analysis. J. Neurosci. Methods 134, 9–21.

Frei, E., Gamma, A., Pascual-Marqui, R., Lehmann, D., Hell, D., Vollenweider, F.X., 2001. Localization of MDMA-induced brain activity in healthy volunteers using low resolution brain electromagnetic tomography (LORETA). Hum. Brain Mapp. 14, 152–165.

Huang, C., Tang, C., Feigin, A., Lesser, M., Ma, Y., Pourfar, M., Dhawan, V., Eidelberg, D., 2007. Changes in network activity with the progression of Parkinson's disease. Brain 130, 1834–1846.

Hughes, A.J., Daniel, S.E., Blankson, S., Lees, A.J., 1993. A clinicopathologic study of 100 cases of Parkinson's disease. Arch. Neurol. 50, 140–148.

Hutchison, W.D., Lozano, A.M., Davis, K.D., Saint-Cyr, J.A., Lang, A.E., Dostrovsky, J.O., 1994. Differential neuronal activity in segments of globus pallidus in Parkinson's disease patients. Neuroreport 5, 1533–1537.

Jeanmonod, D., Magnin, M., Morel, A., 1996. Low-threshold calcium spike bursts in the human thalamus. Common physiopathology for sensory, motor and limbic positive symptoms. Brain 119, 363–375.

Jeanmonod, D., Magnin, M., Morel, A., Siegemund, M., Cancro, R., Lanz, M., Llinás, R., Ribary, U., Kronberg, E., Schulman, J., Zonenshayn, M., 2001. Thalamocortical dysrhythmia II. Clinical and surgical aspects. Thalamus Relat. Syst. 1, 245–254.

Jensen, O., Gelfand, J., Kounios, J., Lisman, J.E., 2002. Oscillations in the alpha band (9–12 Hz) increase with memory load during retention in a short-term memory task. Cereb. Cortex 12, 877–882.

Jones, E.G., 2001. The thalamic matrix and thalamocortical synchrony. Trends Neurosci. 24, 595–601.

Lachaux, J.P., Rodriguez, E., Martinerie, J., Varela, F.J., 1999. Measuring phase synchrony in brain signals. Hum. Brain Mapp. 8, 194–208.

Landolt, H.P., Retey, J.V., Tonz, K., Gottselig, J.M., Khatami, R., Buckelmuller, I., Achermann, P., 2004. Caffeine attenuates waking and sleep electroencephalographic markers of sleep homeostasis in humans. Neuropsychopharmacology 29, 1933–1939.

Llinas, R., 1984. Rebound excitation as the physiological basis for tremor: a biophysical study of the oscillatory properties of mammalian central neurons in vitro. In: Findley, L.J., Capildeo, R. (Eds.), Movement Disorders: Tremor. MacMillan, London, pp. 165–182.

Llinas, R., Pare, D., 1994. The role of intrinsic neuronal oscillations and network ensembles in the genesis of normal and pathological tremors. In: Findley, L.J., Koller, W. (Eds.), Handbook of Tremor Disorders. Marcel Dekker, Inc., New York, NY, pp. 7–36.

Llinás, R., Ribary, U., Jeanmonod, D., Kronberg, E., Mitra, P.P., 1999. Thalamocortical dysrhythmia: a neurological and neuropsychiatric syndrome characterized by magnetoencephalography. Proc. Natl. Acad. Sci. U. S. A. 96, 15222–15227.

Llinás, R., Ribary, U., Jeanmonod, D., Cancro, R., Kronberg, E., Schulman, J., Zonenshayn, M., Magnin, M., Morel, A., Siegemund, M., 2001. Thalamocortical dysrhythmia I. Functional and imaging aspects. Thalamus Relat. Syst. 1, 237–244.

Llinas, R., Urbano, F.J., Leznik, E., Ramirez, R.R., van Marle, H.J., 2005. Rhythmic and dysrhythmic thalamocortical dynamics: GABA systems and the edge effect. Trends Neurosci. 28, 325–333.

Lozano, A.M., Lang, A.E., Hutchison, W.D., Dostrovsky, J.O., 1998. New developments in understanding the etiology of Parkinson's disease and in its treatment. Curr. Opin. Neurobiol. 8, 783–790.

Magnin, M., Morel, A., Jeanmonod, D., 2000. Single-unit analysis of the pallidum, thalamus and subthalamic nucleus in parkinsonian patients. Neuroscience 96, 549–564.

Mitra, P.P., Pesaran, B., 1999. Analysis of dynamic brain imaging data. Biophys. J. 76, 691–708.

Moran, K.A., Schulmann, J.J., Ramirez, R.R., Jaramillo, S., Ribary, U., Llinas, R., 2004. Parkinson's Disease: Thalamocortical Dysrhythmia. Society for Neuroscience, San Diego.

Neufeld, M.Y., Blumen, S., Aitkin, I., Parmet, Y., Korczyn, A.D., 1994. EEG frequency analysis in demented and nondemented parkinsonian patients. Dementia 5, 23–28.

Neuper, C., Pfurtscheller, G., 2001. Event-related dynamics of cortical rhythms: frequency-specific features and functional correlates. Int. J. Psychophysiol. 43, 41–58.

Nichols, T.E., Holmes, A.P., 2002. Nonparametric permutation tests for functional neuroimaging: a primer with examples. Hum. Brain Mapp. 15, 1–25.

Nunez, P.L., Srinivasan, R., 2006. Electric Fields of the Brain. The Neurophysics of EEG Oxford University Press.

Nunez, P.L., Srinivasan, R., Westdorp, A.F., Wijesinghe, R.S., Tucker, D.M., Silberstein, R.B., Cadusch, P.J., 1997. EEG coherency. I: Statistics, reference electrode, volume conduction, Laplacians, cortical imaging, and interpretation at multiple scales. Electroencephalogr. Clin. Neurophysiol. 103, 499–515.

Nunez, P.L., Wingeier, B.M., Silberstein, R.B., 2001. Spatial-temporal structures of human alpha rhythms: theory, microcurrent sources, multiscale measurements, and global binding of local networks. Hum. Brain Mapp. 13, 125–164.

Pascual-Marqui, R.D., Michel, C.M., Lehmann, D., 1994. Low resolution electromagnetic tomography: a new method for localizing electrical activity in the brain. Int. J. Psychophysiol. 18, 49–65.

Pascual-Marqui, R.D., Esslen, M., Kochi, K., Lehmann, D., 2002. Functional imaging with low-resolution brain electromagnetic tomography (LORETA): a review. Methods Find. Exp. Clin. Pharmacol. 24, 91–95 Suppl C.

Pfurtscheller, G., Pichler-Zalaudek, K., Ortmayr, B., Diez, J., Reisecker, F., 1998. Postmovement beta synchronization in patients with Parkinson's disease. J. Clin. Neurophysiol. 15, 243–250.

Salenius, S., Avikainen, S., Kaakkola, S., Hari, R., Brown, P., 2002. Defective cortical drive to muscle in Parkinson's disease and its improvement with levodopa. Brain 125, 491–500.

Sarnthein, J., Jeanmonod, D., 2007. High thalamocortical theta coherence in patients with Parkinson's disease. J. Neurosci. 27, 124–131.

Schnitzler, A., Gross, J., 2005. Normal and pathological oscillatory communication in the brain. Nat. Rev. Neurosci. 6, 285–296.

Silberstein, P., Pogosyan, A., Kuhn, A.A., Hotton, G., Tisch, S., Kupsch, A., Dowsey-Limousin, P., Hariz, M.I., Brown, P., 2005. Cortico-cortical coupling in Parkinson's disease and its modulation by therapy. pp. 1277–1291.

Soikkeli, R., Partanen, J., Soininen, H., Paakkonen, A., Riekkinen Sr., P., 1991. Slowing of EEG in Parkinson's disease. Electroencephalogr. Clin. Neurophysiol. 79, 159–165.

Stanzione, P., Marciani, M.G., Maschio, M., Bassetti, M.A., Spanedda, F., Pierantozzi, M., Semprini, R., Bernardi, G., 1996. Quantitative EEG changes in non-demented Parkinson's disease patients before and during L-dopa therapy. Eur. J. Neurol. 3, 354–362.

Sterio, D., Beric, A., Dogali, M., Fazzini, E., Alfaro, G., Devinsky, O., 1994. Neurophysiological properties of pallidal neurons in Parkinson's disease. Ann Neurol 35, 586–591.

Stoffers, D., Bosboom, J.L., Deijen, J.B., Wolters, E.C., Berendse, H.W., Stam, C.J., 2007. Slowing of oscillatory brain activity is a stable characteristic of Parkinson's disease without dementia. Brain 130, 1847–1860.

Svoboda, J., Sovka, P., Stancak, A., 2004. Effects of muscle contraction on somatosensory event-related EEG power and coherence changes. Neurophysiol. Clin. 34, 245–256.

Tanaka, H., Koenig, T., Pascual-Marqui, R.D., Hirata, K., Kochi, K., Lehmann, D., 2000. Event-related potential and EEG measures in Parkinson's disease without and with dementia. Dement. Geriatr. Cogn. Disord. 11, 39–45.

Timmermann, L., Gross, J., Dirks, M., Volkmann, J., Freund, H.J., Schnitzler, A., 2003. The cerebral oscillatory network of parkinsonian resting tremor. Brain 126, 199–212.

Turner, R.S., Grafton, S.T., McIntosh, A.R., DeLong, M.R., Hoffman, J.M., 2003. The functional anatomy of parkinsonian bradykinesia. Neuroimage 19, 163–179.

Uhlhaas, P.J., Singer, W., 2006. Neural synchrony in brain disorders: relevance for cognitive dysfunctions and pathophysiology. Neuron 52, 155–168.

Volkmann, J., Lado, F., Ioannides, A.A., Mogilner, A., Joliot, M., Ribary, U., Fazzini, E., Llinas, R., 1992. Magnetic recording of resting tremor related brain activity in Parkinson's disease. Soc. Neurosci. Abst. 18, 936s.

Volkmann, J., Joliot, M., Mogilner, A., Ioannides, A.A., Lado, F., Fazzini, E., Ribary, U., Llinas, R., 1996. Central motor loop oscillations in parkinsonian resting tremor revealed by magnetoencephalography. Neurology 46, 1359–1370.